 SDHM, vol.7, no.2, pp.119-137, 2011

Material Uncertainty Effects on Frequency of Composite Plates with Matrix Crack Induced Delaminations

P. Gayathri [1] **and R. Ganguli**[1,2]

Abstract: The effect of random variation in composite material properties on the reliability of structural damage detection is addressed in this paper. A composite plate is considered as the structure and a finite element model is used for the simulation. Damage growth due to cyclic loading is addressed. Matrix crack induced delamination is emphasized in this paper. Thresholds for the damage accumulation are found using finite element simulations so that the structure can be subjected to inspections and removed from service safely. Uncertainty effects of composite material properties on the response of the structure are quantified using Monte Carlo simulations. Vibration modes which are robust damage indicators for fixed and simply supported plates are identified.

Keywords: Composite Structure, Progressive Damage, Delamination, Material Uncertainty

1 Introduction

Composite materials are now widely used in industry. Structures made of composites are susceptible to damage during operation. The damage growth phenomenon in composites is typically more complex than that in metallic structures (Palani, Dattaguru, Nagesh (2008), Robert (2009) and Jeom and Anil (2009)). For example, cyclic loading on composites can result in a complex mechanism of damage growth. Damage detection in composites has become a vital area of research in the last two decades (Della and Shu (2007)). Delamination is one of the primary mechanisms of failure in composites. Delamination in a structure may occur due to many reasons like fabrication defects, in service conditions such as low velocity impact loading etc. Matrix cracking can also become one of the causes of delamination under cyclic loading conditions. Following matrix crack saturation, delamination

[1] Department of Aerospace Engineering, Indian Institute of Science, Bangalore.
[2] Corresponding author. Email: ganguli@aero.iisc.ernet.in, Tel: 91-80-22933017, Fax: 91-80-23600134

can start from the transverse crack tips (Nairn and Hu (1992)). The stiffness of the composite structure reduces significantly due to delamination which directly effects its response and vibration characteristics. Delamination beyond a certain limit may lead to complete failure of the structure.

Typically, progressive damage in composites involves three phases, as shown in Fig. 1. and discussed by Mao and Mahadevan (2002). Here damage index represents the loss of stiffness in the structure with 0 being undamaged and 1 indicating complete damage. In the first phase, there is a rapid stiffness loss and this phase is dominated by matrix cracking. In the second phase, delaminations occur in the structure following matrix crack saturation. Finally, the third phase involves fiber breakage, which is often the final cause of structural failure. From Fig. 1, it can be seen that the point of transition from phase II to phase III is a good point to remove the structure from service or subject it to detailed NDT inspection.

Since it is difficult to measure stiffness degradation, other measurements such as strains and natural frequencies can be used to track the progress of the damage and set appropriate thresholds (Roy and Ganguli (2005)). Mohanty, Chattopadhyay, Wei and Peralta (2009) proposed a new damage index and used an on-line estimation model with an off-line predictive model to adaptively estimate the residual useful life of an AL-6061 cruciform specimen under biaxial loading. Strain gauge sensors were used to estimate the current damage state of the structure. Several recent studies have used modal information to find damage in structures. Giridhara and Gopalakrishnan (2009) derived a damage index using frequency domain strain energy. The method was found to be sensitive for crack detection in rectangular plates and on a compressor blade. Raghuprasad, Lakshmanan, Gopalakrishnan and Muthumani (2008) point out that the reduction in frequencies of a structure due to damage is small. However, frequency reduction is the easiest method for estimating impending damage. Jean-Jacques Sinou (2007) proposed the frequency ratio surfaces intersection method for predicting the location and depth of the crack. He was also able to predict the crack orientation in a circular cross section beam. The crack parameter could be identified by using only the frequency response functions and natural frequency of the cracked structure. Thus, frequencies and strain are useful indicators of damage in structures.

Several works have been conducted on matrix crack induced damage in composites. Kashtalyan and Soutis (2000) found the stiffness degradation in cross ply laminates due to delamination, induced by transverse cracks and splits, using an equivalent constraint model. Shahid and Chang (1995) developed a progressive damage model to predict the accumulated internal damage and its effect on the response of multi-directional composite laminated plates, which is more realistic than cross ply laminates for many structures. Wang and Karihaloo (1997) found

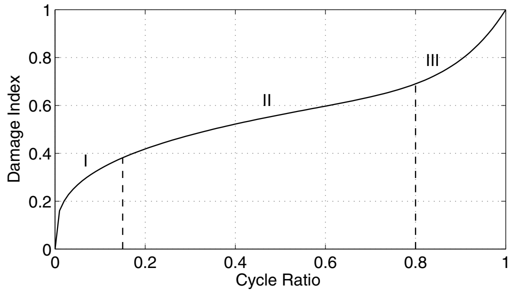

Figure 1: Schematic representation of damage growth in composites

the effect of ply angles on the intensity of delamination induced by matrix cracking. Other recent efforts on progressive damage accumulation in composites are given in (Tay, Tan, Tan and Gosse (2005), Turon, Costa, Maimi, Trias, Mayugo (2005), Zhao and Cho (2007)). Some works have also addressed the fiber breakage damage mechanism (Suyemasu, Kondo , Itatani, Nozue (2001) and Zhang and Thompson (2005)).

In the present study, delamination due to matrix crack accumulation is considered as it is an important failure mechanism for structures under fatigue loading. Following saturation, matrix cracking does not change the effective stiffness of the material. However, cracks will accumulate inside the laminates and weaken the plies, finally leading to other modes of failure like delamination and fibre breakage, which are more critical from the structural failure point of view. Much work has been done on the modeling of matrix cracking, which is generally the initial phase of failure, by various researchers (Sun, Tao, Kaddour (1998), Highsmith and Reifsnider (1982), Laws and Dvorak (1988), Hashin (1985) and Adolfson and Gudmundson (1997)). But, the study on the effects of accumulative damage on realistic structures is limited. Pawar and Ganguli (2006) considered the progressive damage accumulation in a thin-walled composite beam. In another work, Pawar and Ganguli (2007) studied the effect of the damage modes on the structural and aeroelastic response of the rotor blades, taking progressive damage accumulation into consideration. However, these works did not address plate structures. They also did not consider the effect of material property uncertainty on damage detection.

Uncertainty in the material properties is a common phenomenon present in composites, which in turn results in uncertainty in the strength and response characteristics of the structure. Uncertainty can be of two types: aleatory and epistemic (Moens and Vandepitte (2005)). Aleatory or random uncertainty occurs because of randomness in the material properties, geometry, and other properties of the structure. Epistemic uncertainty occurs due to unmodeled physical phenomenon such as transverse shear effects, assumptions in modeling etc. Most work on composite structures focus on reducing the epistemic uncertainty by improving modeling. Much fewer works address aleatory uncertainty. Effect of such aleatory uncertainty must be considered while using damage detection methods so as to get more appropriate results. Literature shows that some researchers have considered the effects of such uncertainties in their analysis (Singh, Yadav, Iyengar, (2001) and Yushanov and Bogdanovich (1998)). Typically, Monte Carlo simulations or stochastic finite element analysis (Mahadevan and Haldar (1991)), can be used to quantify uncertainty effects. However, very few works address the effect of uncertainty in composite material properties on structural damage detection in composites. Reliability aspects of damage detection need to be addressed in research.

In the present work, the Shahid and Chang (1995) model is considered for modeling matrix crack induced delamination caused by cyclic loading. The effect of material property uncertainty on the possibility of detecting the onset of the final phase of damage before failure is considered. Thresholds on the plate deflections and natural frequencies, which can be used to indicate a point where the structure should be removed are given.

2 Composite Plate Model

For a laminated composite plate, the kinematics is governed by the mid-plane displacements u^o, v^o, the transverse displacement w^o and the rotations ψ_x and ψ_y about y and x axes, respectively, as shown in Fig. 2.

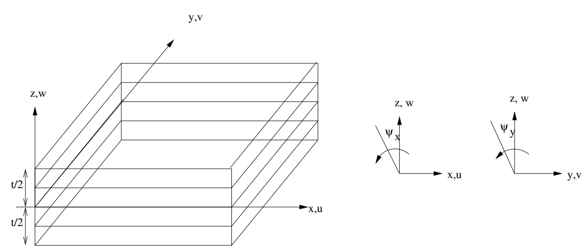

Figure 2: Composite plate under transverse loading

The displacement field is then expressed as

$$u(x,y,z) = u^o(x,y) - z\psi_x(x,y) \tag{1}$$
$$v(x,y,z) = v^o(x,y) - z\psi_y(x,y) \tag{2}$$
$$w(x,y,z) = w^o(x,y) \tag{3}$$

Then, the displacement components u, v and w along x, y and z directions, in terms of midplane nodal degrees of freedom can be expressed as

$$\{u\} = [H]\{\delta\}$$

where, $\{u\} = \{u \;\; v \;\; w\}^T$, $\{\delta\} = \{u^o \;\; v^o \;\; w^o \;\; \psi_x \;\; \psi_y\}^T$ and

$$\{H\} = \begin{bmatrix} 1 & 0 & 0 & -z & 0 \\ 0 & 1 & 0 & 0 & -z \\ 0 & 0 & 1 & 0 & 0 \end{bmatrix}$$

The strains in terms of in-plane and shear strains respectively are

$$\varepsilon = \varepsilon^o + z\kappa \quad \text{and} \qquad \gamma$$

where,

$$\varepsilon^0 = [\varepsilon_x^o \quad \varepsilon_y^o \quad \gamma_{xy}^o]^T = \left[\frac{\partial u^o}{\partial x} \quad \frac{\partial v^o}{\partial y} \quad +\frac{\partial u^o}{\partial y} + \frac{\partial v^o}{\partial x}\right]^T$$

$$\kappa = [\kappa_x \quad \kappa_y \quad 2\kappa_{xy}]^T = \left[-\frac{\partial \psi_x}{\partial x} \quad -\frac{\partial \psi_y}{\partial y} \quad -\frac{\partial \psi_x}{\partial y} - \frac{\partial \psi_y}{\partial x}\right]^T$$

$$\gamma = [\gamma_{yz} \quad \gamma_{xz}]^T = \left[\frac{\partial w^o}{\partial y} - \psi_y \quad \frac{\partial w^o}{\partial x} - \psi_x\right]$$

The stress-strain relationship with respect to x- and y-axis for the k^{th} layer is:

$$\sigma^k = \begin{Bmatrix} \sigma_x \\ \sigma_y \\ \tau_{xy} \end{Bmatrix} = \begin{bmatrix} \bar{Q}_{11} & \bar{Q}_{12} & \bar{Q}_{16} \\ \bar{Q}_{12} & \bar{Q}_{22} & \bar{Q}_{26} \\ \bar{Q}_{16} & \bar{Q}_{26} & \bar{Q}_{66} \end{bmatrix}^k \begin{Bmatrix} \varepsilon_x \\ \varepsilon_y \\ \gamma_{xy} \end{Bmatrix} \tag{4}$$

$$\tau^k = \begin{Bmatrix} \tau_{yz} \\ \tau_{xz} \end{Bmatrix} = \begin{bmatrix} \bar{Q}_{44} & \bar{Q}_{45} \\ \bar{Q}_{45} & \bar{Q}_{55} \end{bmatrix}^k \begin{Bmatrix} \gamma_{yz} \\ \gamma_{xz} \end{Bmatrix} = \bar{C}_s^k \gamma \tag{5}$$

The laminate constitutive relations, that relate the force and moment resultants to the strains are given by

$$\begin{Bmatrix} N \\ M \end{Bmatrix} = \begin{bmatrix} A & B \\ B & D \end{bmatrix} \begin{Bmatrix} \varepsilon^o \\ \kappa \end{Bmatrix} = C_p \varepsilon_p \tag{6}$$

$$\begin{Bmatrix} Q_y \\ Q_x \end{Bmatrix} = \chi \begin{bmatrix} A_{44} & A_{45} \\ A_{45} & A_{55} \end{bmatrix} \begin{Bmatrix} \gamma_{yz} \\ \gamma_{xz} \end{Bmatrix} = C_s \gamma \tag{7}$$

where A, B and D are given by

$$(A_{ij}, B_{ij}, D_{ij}) = \sum_{k=1}^{n} \int_{z_{k-1}}^{z_k} \bar{Q}_{ij}^k (1, z, z^2) dz \quad (i, j = 1, 2, 6) \tag{8}$$

$$A_{ij} = \sum_{k=1}^{n} \int_{z_{k-1}}^{z_k} \bar{Q}_{ij}^k dz \quad (i, j = 4, 5) \tag{9}$$

$\bar{Q}_{ij}^k$ are the elastic constants with respect to x- and y- axis in the global coordinate system for k^{th} layer and χ is the shear correction factor.

2.1 Finite Element Formulation

A finite element model is developed based on the plate theory discussed in the previous section. For discretization, the 4-node Quad elements are used and the element degrees of freedom of this element are

$\delta^e = [\delta_1^e \;\; \delta_2^e \;\; \delta_3^e \;\; \delta_4^e]^T$ and $\delta_i^e = [u_i^o \;\; v_i^o \;\; w_i^o \;\; \psi_{xi} \;\; \psi_{yi}]^T$

Here, δ_i^e represents the nodal degrees of freedom of the midplane. The displacements of the midplane are interpolated by bilinear shape functions. The dynamic equation of the system is

$$[M^e]\{\ddot{\delta}^e\} + [K^e]\{\delta^e\} = \{F^e\} \tag{10}$$

The elemental mass matrix, stiffness matrix and load vector are respectively given by:

$$\begin{aligned} M^e = \int_{V^e} \rho [N]^T [N] dV = \sum_{k=1}^{n} \int_{-1}^{1} \int_{-1}^{1} \rho_k [N]^T \\ \left[\int_{z_k}^{z_{k+1}} [H]^T [H] dz \right] [N] |J| d\xi d\eta \end{aligned} \tag{11}$$

$$K^e = \int_{A^e} (B_b^T C_p B_b + B_s^T C_s B_s) dA = \int_{-1}^{1}\int_{-1}^{1} (B_b^T C_p B_b + B_s^T C_s B_s)|J| d\xi d\eta \tag{12}$$

$$F^e = \int_{A^e} [N]^T \quad f dA = \int_{-1}^{1}\int_{-1}^{1} N^T f |J| d\xi d\eta \tag{13}$$

where, [N] is the shape function matrix, B_b and B_s are strain displacement matrices and f is the distributed force per unit area. A two point Gauss quadrature is used for the numerical integration of mass matrix, bending term of stiffness matrix and force vector, while the shear term of stiffness matrix is integrated using a single point Gauss quadrature. Further details of the finite element formulation can be obtained from (Cen, Soh, Long and Yao (2002) and Lam, Peng, Liu, and Reddy (1997)).

3 Baseline model validation

In order to assess the accuracy of the finite element calculations, a laminated composite plate made of AS4/3501-6 graphite epoxy material with mean values of properties mentioned in Table 1 is considered. Uniformly distributed transverse load is applied on the plate with two different boundary conditions namely, (a) Fixed(clamped-clamped) on two opposite sides and (b) Simply supported on two opposite sides.

For the validation and convergence analysis, the plate considered is of dimensions 200x200x1mm and is made of [0 90 90 0] orthotropic laminates, subjected to a uniformly distributed transverse load of $-100N/m^2$. The convergence of predicted deflection is checked with mesh refinement, considering a square mesh. A 13x13 mesh is found to be sufficient for modeling the composite plate. The results of the converged deflections are then compared with the analytical solutions based on FSDT (Reddy (2000)) in Fig. 3 and are identical.

4 Damage Modeling

In this paper, the damage is assumed to accumulate uniformly in the composite plate. Shahid and Chang (1995) model is used for the damage modeling. This model predicts the accumulated damage in the structure. The damage growth mechanism starts with matrix cracking. Once matrix cracks saturate, the stiffness of the

Plate fixed on two opposite ends

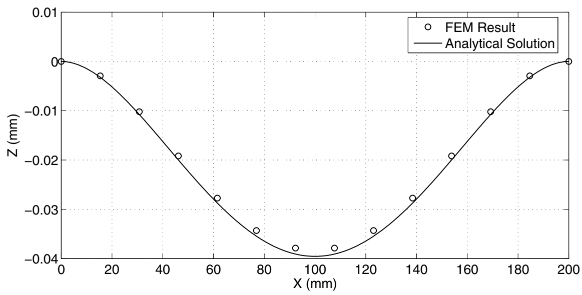

Plate simply supported on two opposite ends

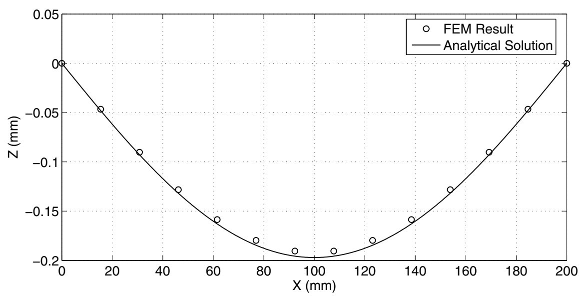

Figure 3: Deflection of composite plate under transverse loading

structure stops reducing at a crack density known as the crack saturation density (ϕ_o). However, matrix cracks tend to induce more severe damage at the tip of the crack such as debonding/delamination.

This transition corresponds to a change from region I to region II in Figure. 1. The material properties of the plate are given in Table 1. The plate considered here is a [45 -45 -45 45] balanced symmetric laminate, with dimensions and loading identical to that mentioned in the previous section.

The effect of the debonding/delamination is modeled at the lamina mechanical property level. Effect of debonding/delamination induced by matrix cracks on the effective by stiffness is estimated based on the continuum damage mechanics approach.The degradation of material properties in a ply due to matrix cracking induced delamination is given by Shahid and Chang (1995).

$$E^d_{xx}(\phi) = E_{xx}(\phi) \tag{14}$$
$$E^d_{yy}(\phi) = E_{yy}(\phi)d_s \tag{15}$$
$$\nu^d_{xy}(\phi) = \nu_{xy}(\phi) \tag{16}$$
$$\nu^d_{yx}(\phi) = \nu_{yx}(\phi)d_s \tag{17}$$
$$G^d_{xy}(\phi) = G_{xy}(\phi)d_s \tag{18}$$

where, d_s is the material degradation factor due to matrix cracking-induced damage, given by

$$d_s = e^{-[\bar{\varepsilon}_{yy}(\phi)/\bar{\varepsilon}_{yy}(\phi_o)]^\eta} \tag{19}$$

where, ϕ_o is the crack saturation density, $\bar{\varepsilon}_{yy}(\phi_o)$ is the effective transverse strain at the saturation crack density and $\bar{\varepsilon}_{yy}(\phi)$ is the transverse strain at a crack density ϕ. Here, η is the material parameter dictating the rate of material degradation due to matrix cracking-induced damage, whose value for graphite/epoxy composites is found to be appropriate at 8 (Shahid and Chang (1995)). $E_{xx}(\phi), E_{yy}(\phi), G_{xy}(\phi)$ and $\mu_{xy}(\phi)$ are the effective mechanical properties including the effect of matrix cracking at crack density ϕ. Since η is constant for a given material, d_s varies with the effective strain strain ratio $(\bar{\varepsilon}_{yy}(\phi)/\bar{\varepsilon}_{yy}(\phi_o))$. In general, the Shahid and Chang model implies that matrix crack induced debonding or delamination damage accumulates with an increase of crack density.

Using the mechanical properties, the ply stiffness due to presence of debonding/delamination can be expressed as,

$$Q^m_{xx}(\phi) = rE^d_{xx}(\phi) \tag{20}$$
$$Q^m_{yy}(\phi) = rE^d_{yy}(\phi) \tag{21}$$
$$Q^m_{yx}(\phi) = r\nu^d_{xy}(\phi)E^d_{xx}(\phi) \tag{22}$$
$$Q^m_{xy}(\phi) = r\nu^d_{yx}(\phi)E^d_{xx}(\phi) \tag{23}$$
$$Q^m_{ss}(\phi) = G_{xy}(\phi)d_s \tag{24}$$

Where

$$r = [1 - \nu_{xy}(\phi)\nu_{yx}(\phi)]^{-1} \tag{25}$$

These equations are used to implement matrix crack induced delamination at the ply level. The matrix crack saturation density is found to be $\phi_o = 3$. The delamination model is integrated into the finite element model and the variation of the transverse modulus with the strain ratio is plotted as shown in Fig 4.

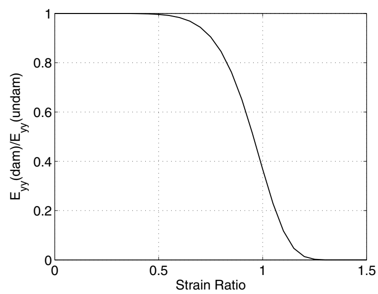

Figure 4: Variation of the transverse modulus with strain ratio

From Fig. 4, it can be seen that there is a significant change in the transverse modulus between the strain ratio of 0.5 and 1.25. Based on the loss of threshold material stiffness, the likelihood of failure due to delamination is high after a strain ratio of 1.25 (Pawar and Ganguli (2007)). Also, the maximum deflection of the composite plates at matrix crack saturation corresponds to a value of strain ratio of about 1. This was identified in an earlier work by Pawar and Ganguli (2007) who also suggested that this point could be used to create a threshold for the structure to be subject to detailed NDT inspections. The logic here is that a structure rarely fails by matrix cracking but its saturation is the trigger for delamination induced failure. So in further studies, the effect of delamination is considered to take place between the strain ratios of 1 and 1.25. Note that the results in this paper correspond to matrix crack induced delamination/debonding which follows matrix crack saturation.

Fig. 5 shows the effect of delamination on the deflection of the composite plates. Plots in the left column of Fig. 5 show the variation of the maximum deflection of various plates with the strain ratio. As can be observed from these plots, the deflection increases with increase in the strain ratio i.e, damage, as expected. The increase is drastic after a strain ratio of around 1.25. This implies that beyond this value of strain ratio, the structure will fail, which can also be observed from the stiffness degradation in Fig. 4. The strain ratio of 1.25 marks the beginning of rapid loss of stiffness before final failure and the values of deflection and other system parameters at this point can be used as a threshold for removal of the structure from service. So, the value of strain ratio of 1.25 is taken as the point of maximum

Fixed on two opposite ends

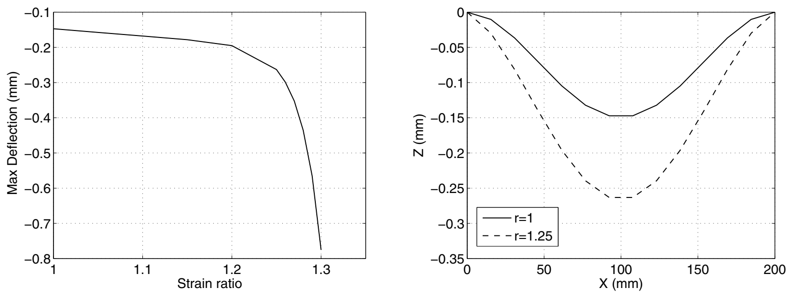

Simply supported on two opposite ends

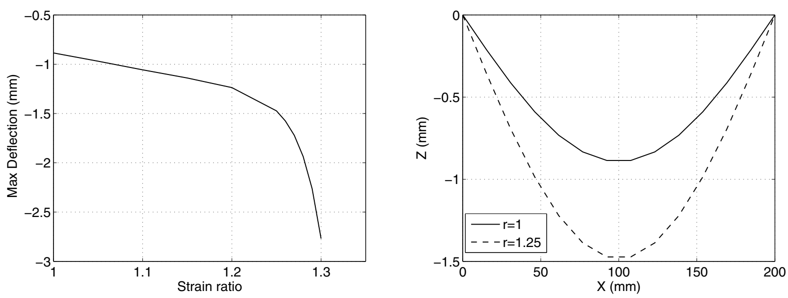

Figure 5: Effect of delamination on the deflection of the plates

delamination before final failure and the analysis is done, considering this value. The right side plots of Fig. 5 are the deflection curves for the two strain ratio values of 1 and 1.25.

Table 2 gives the maximum deflection and the first five natural frequencies of the plates at the strain ratio of 1.25 and also their percentage change due to delamination for the strain ratio increasing from 1 to 1.25. It can be seen that significant changes in the maximum deflections occur due to delamination when compared to the matrix crack saturated plate.

5 Monte Carlo Simulations

Monte Carlo simulations are done to account for material property uncertainty. The threshold limit for delamination is taken at the strain ratio of 1.25. 5000 Monte Carlo runs are simulated for the plates with the material properties and their coefficients of variations as given in Table-1. The coefficient of variation is defined as the ratio of the standard deviation to the mean, for a Gaussian random variable. The elastic material properties of the composite material $(E_{xx}, E_{yy}, E_{zz}, G_{xy}, G_{xz}, G_{yz}, r_{xy})$ are treated as random variables. A Gaussian distribution is considered for each random variable. Such a random variable x_i is given by

$$x_i = \mu_0 + \sigma_0 r_i \tag{26}$$

where μ_0 is the mean, σ_0 is the standard deviation and r_i is any random number generated form a Gaussian distribution with a mean of 0 and a standard deviation of 1. The results of natural frequencies of these simulations are given in Fig. 6-7 for the undamaged plate, matrix crack saturated plate (r=1) and delaminated plate (r=1.25). The matrix crack results correspond to matrix crack saturation and to the transition from phase I to phase II in Fig. 1. Since structures typically do not fail by matrix cracking, the transition from phase I to phase II can be considered as the point where the structure should be monitored more closely. The second threshold corresponds to transition from phase II to phase III and represents the point where the structure should be removed or subjected to major inspections. These two thresholds serve as valuable indicators of the health of the composite structure.

The plots for the first five natural frequencies are shown in the Figs. 6-7. The plots in the left column show the probability distribution of the natural frequencies for the three damage cases from right to left i.e, undamaged, damage by matrix cracking saturation and significant damage due to delamination, respectively. The right side plots show the probability distribution curves for the left side plots along with the deterministic values. For the fixed plate results in Figs. 6, the undamaged plates are clearly separated from the damaged delaminated plate for all the five modes. However, there is consider overlap between the frequencies of the matrix crack saturated plate and the undamaged plate. Mode 1 appears useful for separating the undamaged plate from the matrix crack saturated plate. Here, modes 4 and 5 appear good for separating the matrix crack saturation point from the delamination end point.

For the simply supported plates in Fig. 7, there is some overlap between the matrix crack saturated plate and the delaminated plate. However, the delaminated plate is completely separated from the undamaged plate. Mode 1 offers good separation between the undamaged and matrix crack saturated plates. Mode 5 offers good separation between the matrix crack saturated and delaminated plate.

These results are summarized in Table 3. The first mode is a robust indicator for identifying the transition between the undamaged plate and the matrix crack saturated plate. For the point of substantial delamination, the higher modes such as the fifth mode are most robust to uncertainty. Note that modal based methods may not be able to detect small cracks. However, most aerospace structures are designed to tolerate a substantial amount of damage (Boller (2000), Cattarius and Inman (2000)). Modal methods are not very susceptible to false alarms due to their insensitivity to small damage. Thus, modal parameters are useful for global decision on when to put a structure on watch for more detailed monitoring for their removal. The decision of removal is expensive and should be taken only when substantial amount of deterioration has taken place.

A probabilistic analysis can identify which damage indicators(for example, modes) are less susceptible to structure uncertainty and therefore a better choice for damage detection. The thresholds developed in this paper can be very useful for health monitoring as they are robust to the presence of material uncertainty. Though the result in this study apply for the specific damage model used, other damage models and more realistic structures can also be considered.

Table 1: Material properties and uncertainty indicators of AS4/3501-6 graphite epoxy

Ply Property	Mean Value	% Coeff. of variation (Vinckenroy and Wilde (1995))
Longitudinal Modulus, E_{xx}, GPa	141.96	3.39
Transverse Modulus, E_{yy}, GPa	9.79	4.27
Transverse Modulus, E_{zz}, GPa	9.79	4.27
In-plane shear modulus, G_{xy}, GPa	6	4.27
Transverse shear modulus, G_{xz}, GPa	6	4.27
Transverse shear modulus, G_{yz}, GPa	2.5	4.27
Poisson's ratio, ν_{xy}	0.42	3.65
Density, ρ, kg m^{-3}	1600	0

6 Conclusion

The effect of progressive damage in composites is considered. A finite element model of a two different composite plates is used for the numerical results. The effect of matrix crack induced delamination in composites on the plate response is studied. The transition point between delamination and fiber breakage is identified as the best location where the structure should be removed. The saturation of matrix cracking is a good point to start observing the structure closely. Monte Carlo

Natural Frequency-1

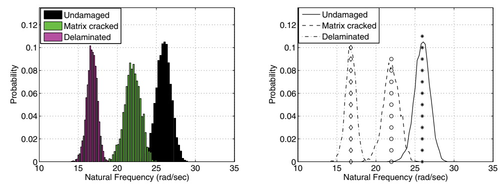

Natural Frequency-2

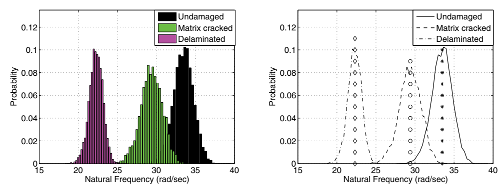

Natural Frequency-3

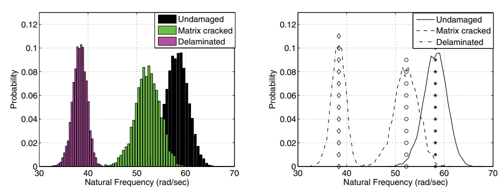

Natural Frequency-4

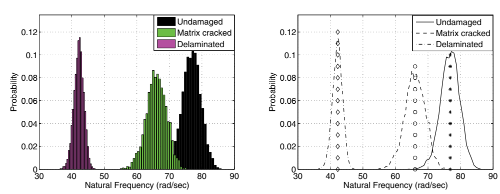

Natural Frequency-5

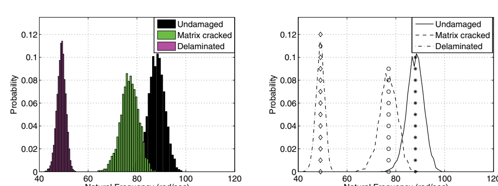

Figure 6: Effect of significant delamination and matrix crack saturation on the natural frequencies of plate fixed on opposite ends

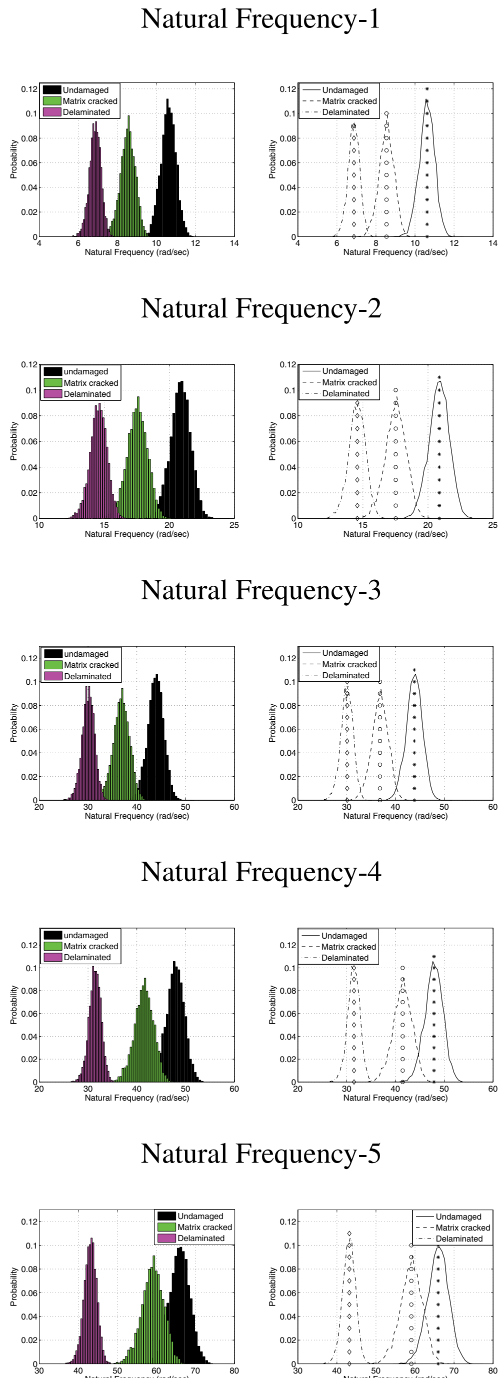

Figure 7: Effect of significant delamination and matrix crack saturation on the natural frequencies of plate simply supported on opposite ends

Table 2: Values of deflection (mm) and natural frequencies (rad/s) at strain ratio 1.25 (significant delamination) and their percentage change (in brackets) for the strain ratio varying from 1 (matrix crack saturation) to 1.25

Plate Type	Deflection	NF1	NF2	NF3	NF4	NF5
Fixed	-0.263(78.74)	16.611(25.98)	22.19(25.67)	38.216(27.44)	41.493(36.5)	48.5(36.48)
SSB	-1.473(83.37)	6.835(24.18)	14.523(20.2)	29.907(21.52)	31.096(25.82)	42.883(27.65)

Table 3: Modes suitable for damage monitoring under uncertainty

Plate Type	Undamaged to Crack Saturation Transition (Put structure on watch)	Substantial Delamination and Debonding (remove structure)
Fixed	1	4, 5
Simply Supported	1	5

simulations are run, taking 5000 points to consider the material property uncertainties. It is found that the undamaged and the delaminated plate are clearly separated. However, modes 1 and 4 are useful for separate the matrix cracked and delaminated modes for the fixed plates. Modes 1, 4 and 5 are good for represent matrix cracked plate and delaminated plate for the simply supported plates.

References

Adolfsson, E.; Gudmundson, P. (1997): Thermoelastic properties in combined bending and extension of thin composite laminates with transverse matrix cracks, *Int. J. Solids Structures*, Vol. 34, No. 16, pp. 2035-2060.

Boller, C. (2000): Next generation structural health monitoring and its integration into aircraft design, *International Journal of Systems Science*, Vol. 31, No. 11, pp. 1333-1349.

Cattarius, J.; Inman, D. J. (2000): Experimental verification of intlligent fault detection in rotor blades, *International Journal of Systems Science*, Vol. 31, No. 11, pp. 1375-1379.

Cen, S.; Soh, A. K.; Long, Y. Q.; Yao, Z. (2002): A new 4-node quadrilateral FE model with variable electrical degrees of freedom for the analysis of piezoelectric laminated composite plates, *Composite Structures*, Vol. 58, No. 4, pp. 583-599.

Della, C. N.; Shu, D. (2007): Vibration of delaminated composite laminates: A review, *Transactions of ASME: Applied Mechanics Reviews*, Vol. 60, pp. 1-20.

Giridhara, G.; Gopalakrishnan, S. (2009): Frequency Domain based Damage Index for Structural Health Monitoring, *Structural Durability and Health Monitoring*, Vol. 5, No. 1, pp. 1-32.

Hashin, Z. (1985): Analysis of cracked laminates: A variational approach, *Mechanics of Materials*, Vol. 4, pp. 121-136.

Highsmith, A. L.; Reifsnider, K. L. (1982): Stiffness Reduction Mechanics in Composite Laminates. Damage in Composite Materials, *American Society for Testing and Materials, New York*, Vol. 775, pp. 103-117.

Kashtalyan, M.; Soutis, C. (2000): The effect of delaminations induced by transverse cracks and splits on the stiffness properties of composite laminates, *Composites Part A-Applied Science and Manufacturing* Vol. 31, No. 2, pp. 107-119.

Klaasen, H.; Kubarsepp, J. (2007): Performance of carbide composites for cyclic loading applications, *International Journal of Materials and Product Technology*, Vol. 28, No. 3-4, pp. 399-424.

Lam, K. Y.; Peng, X. Q.; Liu, G. R.; Reddy, J. N. (1997): A finite-element model for piezoelectric composite laminates, *Smart Materials and Structures*, Vol. 6, No. 5, pp. 583-591.

Laws, N.; Dvorak, G. J. (1988): Progressive transverse cracking in composite laminates, *Journal of Composite Materials*, Vol. 22, No. 10, pp. 900-916.

Mahadevan, S.; Haldar, A. (1991): Practical random field discretization in stochastic finite element analysis, *Structural Safety*, Vol. 9, No. 4, pp. 283-304.

Mao, H.; Mahadevan, S. (2002): Fatigue damage modelling of composite materials, *Composite Structures*, Vol. 58, No. 4, pp. 405-410.

Mohanty, S.; Chattopadhyay, A.; Wei, J.; Peralta, P. (2009): Real Time Damage State Estimation and Condition Based Residual Useful Life Estimation of a Metallic Specimen under Biaxial Loading, *Structural Durability and Health Monitoring*, Vol. 5, No. 1, pp. 33-36.

Moens, D.; Vandepitte, D. (2005): A survey of non-probabilistic uncertainty treatment in finite element analysis, *Comput. Methods Appl. Mech. Engrg*, Vol. 194, No. 12-16, pp. 1527-1555.

Nairn, J. A.; Hu, S. (1992): The initiation and growth of delaminations induced by matrix microcracks in laminated composites, *International Journal of Fracture*, Vol. 57, No. 1 , pp. 1-24.

Paik, J. K.; Thayamballi, A. K. (2009): Recent Advances and Fututre Trends on Design and Strength Assessment of Ships and Offshore Structure, *Structural*

Longevity, Vol. 1, No. 1, pp. 37-60.

Palani, G, S.; Dattaguru, B.; Nagesh, R. Iyer. (2008): A Generalized Technique for Fracture Analysis of 2-D Crack Problem Employing Sigular Finite Elements , *Structural Durability and Health Monitoring*, Vol. 4, No. 2, pp. 77-94.

Pawar,P. M .; Ganguli, R. (2006): Modelling progressive damage accumulation in thin walled composite beams for rotor blade applications, *Composites Science and Technology*, Vol. 66, No. 13, pp. 2337-2349.

Pawar, P.M.; Ganguli, R. (2007): On the effect of progressive damage on composite helicopter rotor system behavior, *Composite Structures*, Vol. 78, No. 3, pp. 410-423.

Raghuprasad, B, K.; Lakshmanan, N.; Gopalakrishnan, N.; Muthumani, K.; (2008): Sensitivity of Eigen Values to Damage and Its Identification, *Structural Durability and Health Monitoring*, Vol. 4, No. 3, pp. 117-144.

Reddy, J. N. (2000): Mechanics of Laminated Composite Plates, *CRC Press, Boca Raton, Florida*.

Robert, E. Melchers. (2009): Validity and Quality of Deterioration Models for Structural Reliability Assessment, *Structural Longevity*, Vol. 5, No. 1, pp. 1-32.

Roy, N.; Ganguli, R. (2005): Helicopter rotor blade frequency evolution with damage growth and signal processing, *Journal of Sound and Vibration*, Vol. 283, No. 3-5, pp. 821-851.

Shahid, I.; Chang, F. K. (1995): An accumulative damage model for tensile and shear failures of laminated composite plates, *J Compos Mater*, Vol. 29, No. 7, pp. 926-981.

Singh, B. N.; Yadav, D.; Iyengar, N.G.R. (2001): Natural frequencies of composite plates with random material properties using higher order shear deformation theory, *International Journal of Mechanical Sciences*, Vol. 43, No. 10, pp. 2193-2214.

Sinou, J. J. (2009): Damage Assessment Based on the Frequencies' Ratio Surfaces Intersection Method for the Identification of the Crack Depth, Location and Orientation, *Structural Durability and Health Monitoring*, Vol. 3, No. 3, pp. 133-164.

Sun, C. T.; Tao, J.; Kaddour, A. S. (1998): Prediction of failure envelopes and stress/strain behavior of composite laminates, *Composites Science and Technology*, Vol. 58, No. 7, pp. 1125-1136.

Suyemasu, H.; Kondo , A.; Itatani, K.; Nozue, A. (2001): A probabilistic approach to the toughening mechanism in short-fiber-reinforced ceramic matrix composites, *Composites Science and Technology*, Vol. 61, No.2, pp. 281-288.

Tay, T. E.; Tan, S. H. N.; Tan, V. B. C.; Gosse, J. H. (2005): Damage progression by the element- failure method (EFM) and strain invariant failure theory (SIFT), *Composites Science and Technology*, Vol. 65, No. 6, pp.935-944.

Turon, A.; Costa, J.; Maimi, P.; Trias, D.; Mayugo, J. F. (2005): A progressive damage model for unidirectional fibre-reinforced composites based on fibre fragmentation. Part I:Formulation, *Composites Science and Technology*, Vol. 65, No. 14, pp. 2039-2048.

Viadero, F.; Bueno, J. l.; Delacalle, L. N. L.; Sanchibrian, R. (1994): Reliability computation on stiffened bending plates, *Advances in Engineering Software*, Vol. 20, No. 1, pp. 43-48.

Vinckenroy, G. V.; Wilde, W. P. De. (1995): The Use of Monte Carlo Techniques in Statistical Finite Element Methods for the Determination of the Structural Behaviour of Composite Materials Structural Components, *Composite Structures*, Vol. 32, No. 1-4, pp. 247-253.

Wang, J.; Karihaloo, B. L. (1997): Matrix crack-induce delamination in composite laminates under transverse loading, *Composite Structures*, Vol. 38, No. 1-4, pp. 661-666.

Yushanov, S. P.; Bogdanovich, A. E. (1998): Analytical probabilistic modeling of initial failure and reliability of laminated composite structures, *Int. J. Solids Structures*, Vol. 35, No. 7-8, pp. 665-685.

Zhang, G.; Thompson, M.R. (2005): Reduced fibre breakage in a glass-fibre reinforced thermoplastic through foaming, *Composites Science and Technology*, Vol. 65, No. 14, pp. 2240-2249.

Zhao, G. P.; Cho, C. D. (2007): Damage initiation and propogation in composite shells subjected to impact, *Composite Structures*, Vol. 78, No. pp. 91–10